

StationRank: Aggregate dynamics of the Swiss railway

Georg Anagnostopoulos^{1*}, Vahid Moosavi²

1 Independent Researcher, Zurich, Switzerland

2 Department of Architecture, ETH Zurich, Zurich, Switzerland

* Corresponding author

E-mail: mail@anagno.com (GA)

Abstract

Increasing availability and quality of actual, as opposed to scheduled, open transport data offers new possibilities for capturing the spatiotemporal dynamics of railway and other networks of social infrastructure. One way to describe such complex phenomena is in terms of stochastic processes. At its core, a stochastic model is domain-agnostic and algorithms discussed here have been successfully used in other applications, including Google’s PageRank citation ranking. Our key assumption is that train routes constitute meaningful sequences analogous to sentences of literary text. A corpus of routes is thus susceptible to the same analytic tool-set as a corpus of sentences. With our experiment in Switzerland, we introduce a method for building Markov Chains from aggregated daily streams of railway traffic data. The stationary distributions under normal and perturbed conditions are used to define systemic risk measures with non-evident, valuable information for operation and planning.

Introduction

We study the dynamics of the Swiss railway network over a period of one month via characteristics of Markov Chains (MCs) [15]. Originally conceived for statistical analysis of texts, MCs have proven useful in various fields such as search engines [18], traffic dynamics [7, 12, 16] and econometrics [2, 17]. More formally, MCs are defined as stochastic processes that display the *Markov Property*

$$p(x_{k+1} = S_{k+1} | x_k = S_k, x_{k-1} = S_{k-1}, \dots, x_0 = S_0) = p(x_{k+1} = S_{k+1} | x_k = S_k), \quad (1)$$

which means that the probability of a random variable x being at state S_{k+1} at time step $k + 1$ only depends on its state at time step k [7]. We found that, for the Swiss railway, a time step of 1 minute is appropriate. Bigger time steps might lead to spatial ambiguities and are not valid without sampling in Euclidean space [16].

Overall, we have a day-to-day dynamic process, where each day is one discrete-time, finite-state homogeneous MC [7, 16] for itself. In a way, we have 2 levels of aggregation and discretization [9]: days within a month and minutes within a day. Because trains at a given minute might be either at some station or in transit between stations, our finite states include real stations and also virtual transit states. Here is an example of one route as state transition sequence:

Example 1. *StationA, StationA-StationB, StationA-StationB, StationB, StationB, StationB-StationC, ..., StationY-StationZ, StationZ*

Every MC can be stored in the form of a row-stochastic non-negative $n \times n$ *transition probability matrix* \mathbb{P} , where n is the number of states and \mathbb{P}_{ij} is the transition probability from state S_i to state S_j [7]. Each state corresponds to a node of a directed graph \mathcal{G} and each state-transition corresponds to an edge. Diagonal entries of \mathbb{P} can be represented as self-loops in \mathcal{G} . As \mathbb{P} is row-stochastic, the elements of each row should sum up to 1 [7]. Because the number of actual station states and also the number of virtual transit states is subject to daily variation, the size of the corresponding MC also varies, Fig 1. In order to ensure comparability, we define a common intersection of actual stations. At a coverage of 75% of the Swiss railway, this equals 1194 stations.

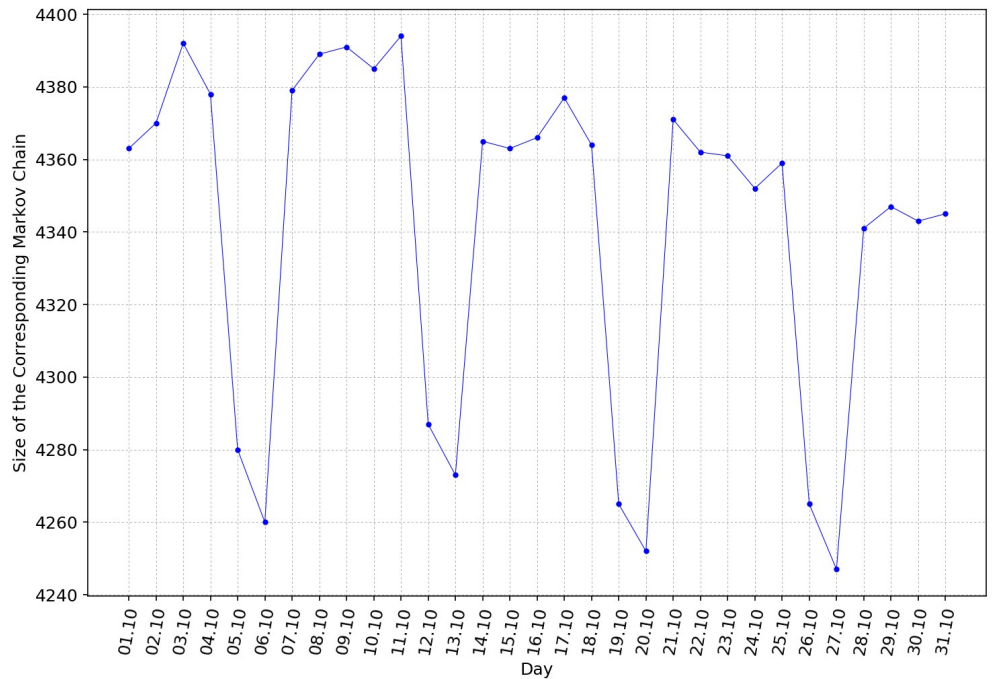


Figure 1. Size of the corresponding Markov Chain, October 2019

A clear weekly pattern can be observed. MCs on Saturdays and Sundays are smaller.

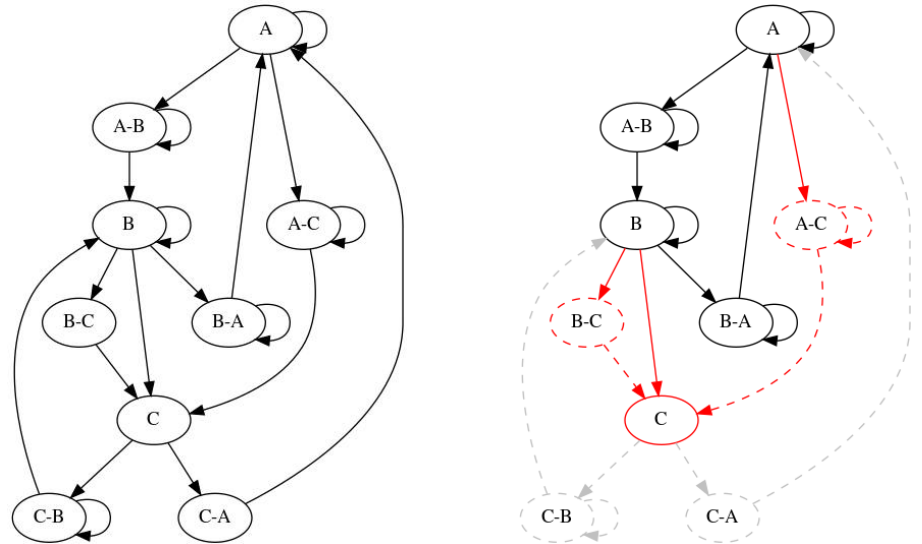
The Data

The actual data [11] is published by the Swiss Federal Railways (SBB) on a daily basis. In contrast to timetables, each day of actual data is a unique collection of routes that enables us to study the real behavior of the network. The data set is multi-modal, including trains, buses, trams, metro and boats. In the present work we take only railway traffic into consideration under the assumption that the corresponding networks are of different nature: trains do not typically share stations with boats and have also very different speed. The data set is also multi-jurisdictional, involving many different operators, a challenging setup from the perspective of homogeneity and data integrity.

Most of the methods developed around linear dynamical systems are based on discrete-time and homogeneous MCs. This means that continuous dwell and running times [12] need to be discretized [9] as a kind of preprocessing step. The result is a series of $N \times 1440$ matrices, where N is the number of executed routes on the said day and 1440 is the total number of discrete steps (minutes). Generally, the actual data is a valuable source also for other investigations such as spatio-temporal prediction problems.

The Model

We propose here a hybrid model which combines features of both **primal** and **dual** networks [7, 13, 19]. A primal approach would represent stations as nodes and their connections as edges. The inverse, dual approach would turn the connections into nodes and the stations into edges. Primal networks are typically graphed in L-space [4, 21] and the respective graphs can be either planar [10, 16] or non-planar. The planar case is often referred to as **space-of-stations** where the links play the role of physical rail-tracks, while the non-planar as **space-of-stops** [13, 21] where the links connect consecutive stops of a route. Dual networks are typically graphed in P-space [4, 13, 21], also referred to as **space-of-changes** [13] or **space-of-transfer** [21]. The advantages or drawbacks of primal and dual have already been thoroughly discussed in other works [7, 13, 19], but, to our best of knowledge, merging the two modes offers an alternative perspective that has not enjoyed enough attention yet. Thus, we introduce a generic **space-of-states**, where a state can be a stop or a transit, Fig 2a. A space of states explicitly captures temporal dynamics as it does not assume any fixed topology (e.g. roads or rail-tracks) and can be implemented as a discrete-time, finite-state homogeneous MC without spatial sampling. This novel approach is easily applicable to other systems, such as air traffic.



(a) MC as directed graph with self-loops (b) Disruption at C - perturbation strategy

Figure 2. Model architecture

Stations might be directly or indirectly connected via transit states.

Building ergodic MCs

For every day, we assume a *strongly connected* directed graph \mathcal{G} which also implies that the corresponding matrix \mathbb{P} should be *irreducible* [7, 16]. All states of an irreducible and aperiodic MC, commonly referred to as *ergodic*, are **positive recurrent** [20] with

$$\mathbb{E}(T_i | x_0 = S_i) < \infty, \quad (2)$$

where T_i is the time of first return to S_i . This means that a traveler is expected to return to an initial state within a finite number of steps.

Matrices built from actual data don't always contain only positive recurrent states. There are two kinds of states which need special attention: **null-recurrent** [16, 20] and **absorbing states** [1, 17, 18].

- State S_i is null-recurrent if $\mathbb{E}(T_i|x_0 = S_i) = \infty$
- State S_i is absorbing if $p(x_{k+1} = S_i|x_k = S_i) = 1$

Essentially, returning to a null-recurrent or escaping from an absorbing state is impossible. In order to solve this problem, we use the technique of teleportation according to which the Markov matrix can be updated as follows:

$$\hat{\mathbb{P}}_{ij} = \alpha \mathbb{P}_{ij} + (1 - \alpha)/n, \quad (3)$$

where $0 < \alpha < 1$ is the teleport probability [16]. Table 1 provides an overview of the stations that were found to behave either as null-recurrent or as absorbing states.

Table 1. Actual null-recurrent and absorbing states, October 2019

Notice that most of these states are border stations. Interestingly, on 29.10 both null-recurrent and absorbing states were observed. Here the absorbing state is a depot and the null-recurrent belongs to a brand new line, officially launched two months later.

Date	Null-recurrent	Absorbing
03.10		Chiasso Olimpino I
04.10	Landesgrenze CH-Liechtenstein	
07.10	Schaffhausen Nord	
08.10		Sagliaains Abzw Sasslatschtunne
11.10	Schaffhausen Nord	
15.10	Genève-Stade	
17.10		Gaggiolo Confine
20.10		La Plaine-Frontière
21.10	Gaggiolo Confine La Plaine-Frontière Landesgrenze CH-Liechtenstein	
23.10		Le Locle-Frontière
29.10	Chêne-Bourg	Genève Voie-Creuse

Eigenspectra and the Kemeny constant

For every ergodic MC, according to the Perron-Frobenius theorem [7, 16], all eigenvalues of \mathbb{P} are within a *spectral radius* of 1 with the largest of them, called the *Perron root*, being always equal to 1 and unique. The corresponding left-hand Perron eigenvector is also unique and defined by

$$\pi^T \mathbb{P} = \pi^T, \quad (4)$$

such that $\pi > 0$ and $\|\pi\|_1 = 1$. Each entry π_i of the *stationary distribution vector* π^T represents the long-run time fraction of being in the respective state [7]. Of particular interest is also the second eigenvector of \mathbb{P} . It has been shown [7, 14] that if the respective eigenvalue is real, it associates nodes to weakly-connected sub-communities.

Given the eigenvalues $\lambda_1 = 1, \lambda_2, \dots, \lambda_n$, we can compute the *Kemeny constant* K which is an intrinsic quantity of every MC [7, 16, 17].

$$K = \sum_{j=2}^n \frac{1}{1 - \lambda_j}, \quad (5)$$

K can be interpreted as the average expected time (steps) from any given state (origin) to any other random state (destination). As such, it is an excellent indicator of network connectivity and it can be used to evaluate the impact of modifications on the overall performance of the network [16, 17]. To obtain the average travel time in minutes, the constant should be divided by the time-frame of aggregation which in our case is 1440 minutes. For the Swiss railway network, we calculated that $K \approx 30.5, \pm 1$ minute.

Sensitivity analysis of transition probability matrices

At least two methodologies for robustness assessment of the Swiss railway network under perturbed conditions have been proposed in the past: graph-theoretical and aggregated. The graph-theoretical approach [8], attempts to establish a structural and operational robustness assessment framework, but does not include dynamic aspects. The aggregated [6] approach explains the spatio-temporal ramifications of an extremely rare disruptive event in statistical terms, but has a rather forensic than operational character. Here we choose a data-driven and aggregated perturbation methodology in the form of sensitivity analysis of transition probability matrices. Our approach is able to scale and has the potential to be applied, beyond the national, to a continental level.

It has been shown in previous works [16, 17] that, by perturbing the values of the corresponding transition matrix, one can analyze the effect of a disruption at some node on the other nodes and the network as a whole. The original transition matrix \mathbb{P} is thus perturbed into $\tilde{\mathbb{P}} = \mathbb{P} + E$ [7], where E is a singular matrix (each row sums to 0). For a reduction of just one entry \mathbb{P}_{ip} of the Markov matrix by a quantity $t \cdot \mathbb{P}_{ip}$

$$E = t \frac{\mathbb{P}_{ip}}{1 - \mathbb{P}_{ip}} \mathbf{e}_i [\mathbf{e}_i^T \mathbb{P} - \mathbf{e}_p^T], \quad (6)$$

where \mathbf{e}_k is a vector whose k^{th} entry equals 1 [7] and $\mathbb{P}_{ip} < 1$. If $\mathbb{P}_{ip} = 1$, then $E_{ip} = -t$, $E_{ii} = t$ and all other entries of E are set to 0. In order to linearly reduce the activity of a certain station (node) [17], we need to perform the above perturbation on multiple incoming edges of direct or indirect connection to that station, Fig 2b. If the connection is bi-modal (direct and indirect), then Eq (6) can be generalized for a finite set of nodes:

$$E = t \frac{\sum_{j \in S} \mathbb{P}_{ij}}{1 - \sum_{j \in S} \mathbb{P}_{ij}} \mathbf{e}_i [\mathbf{e}_i^T \mathbb{P} - \mathbf{e}_S^T], \quad (7)$$

where every j^{th} entry of \mathbf{e}_S equals $\frac{\mathbb{P}_{ij}}{\sum_{j \in S} \mathbb{P}_{ij}}$ and $\sum_{j \in S} \mathbb{P}_{ij} < 1$.

Linear reduction of a station's activity by multiple perturbations of the transition probability matrix is more suitable for a real-world network than simple node removal. Our strategy to indirectly cause the disruption by weakening the incoming links allows also for plenty of variation and flexibility. We assumed a homogeneous reduction of 95% on all incoming links, but any percentage, link subset, or random linear combinations, are valid options. The algorithm can be adjusted also for perturbation on the outgoing links, depending on the scope of application.

From the resulting perturbed transition probability matrix $\tilde{\mathbb{P}}$, a new stationary distribution $\tilde{\pi}$ can be calculated. Along with the assessment of the perturbation's impact on network performance metrics, such as the Kemeny constant, dedicated systemic risk measures can be articulated by comparing the stationary distributions under normal and perturbed conditions.

Results

The methodology we proposed here is generic and can account for different use cases. Therefore, we highlight few of them that we found interesting for the reader. Even in a highly efficient, optimized and well studied system such as the Swiss railway network, there are surprising results when dealing with the daily variation of the actual flows. We will explain the results on different levels of abstraction and detail.

First Eigenvector

The first eigenvector of the transition probability matrix \mathbb{P} is equivalent to the stationary distribution of the system. In terms of traffic networks, each vector component π_i measures congestion at the corresponding station [7, 16], Fig 3.

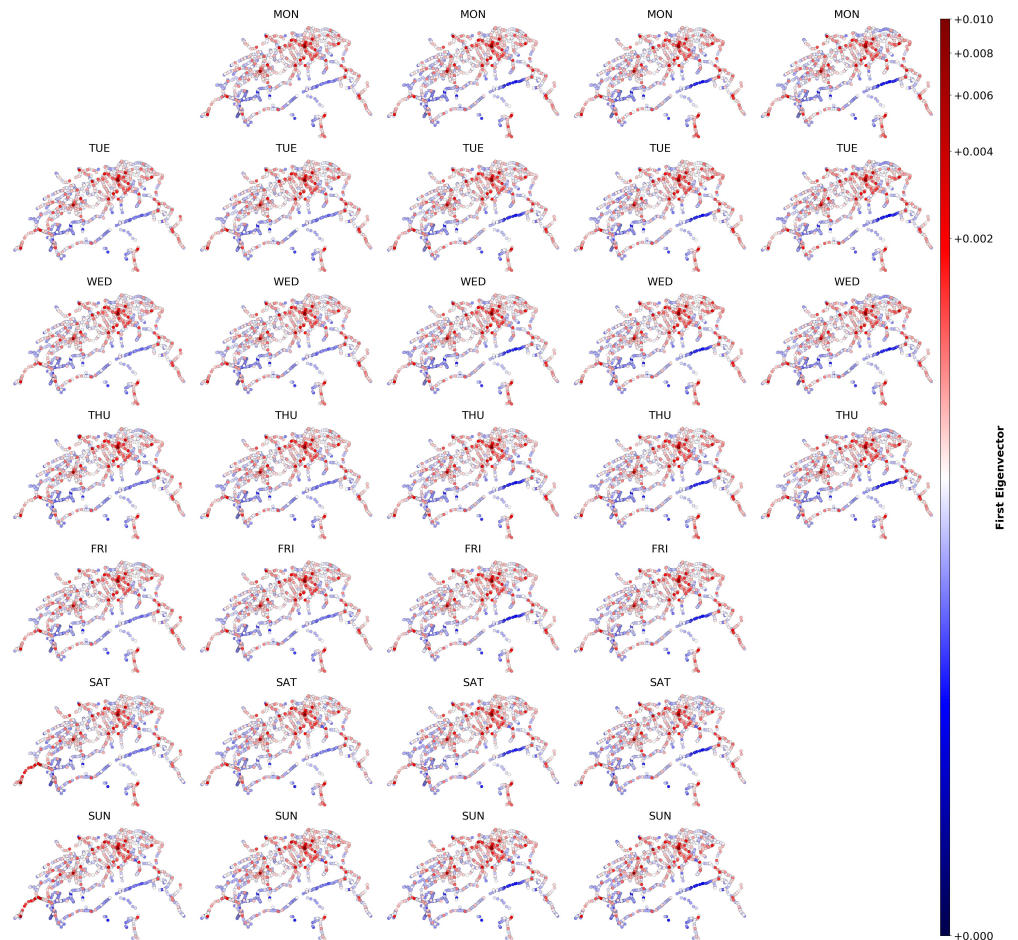


Figure 3. Time series of the stationary distribution (1st Eigenvector)
Evolution of the stationary distribution for the Swiss railway network in October 2019. A segment of the lowest probabilities is further reduced towards the end of the month.

The first eigenvector provides a high level overview of the system and remains largely stable with time. Nevertheless, closer inspection reveals certain trends. In the first weekend, high probabilities were redistributed in the west part of the country. Furthermore, some of the lowest probabilities were reduced near the end of the month. For more details and variation, we also need to consult the second eigenvector.

Second Eigenvector

Due to the orthogonality of first and second eigenvector, there is zero correlation between them and thus both convey very valuable and non overlapping information. Whereas the first one is equivalent to the stationary distribution, the second one is related to the second eigenvalue which measures the rate of convergence to the stationary distribution [7]. As we mentioned before, the second eigenvector is known to be a good indicator for the existence of weakly-connected sub-communities and is closely related to the concept of spectral clustering and minimum balanced cuts [14], Fig 4.

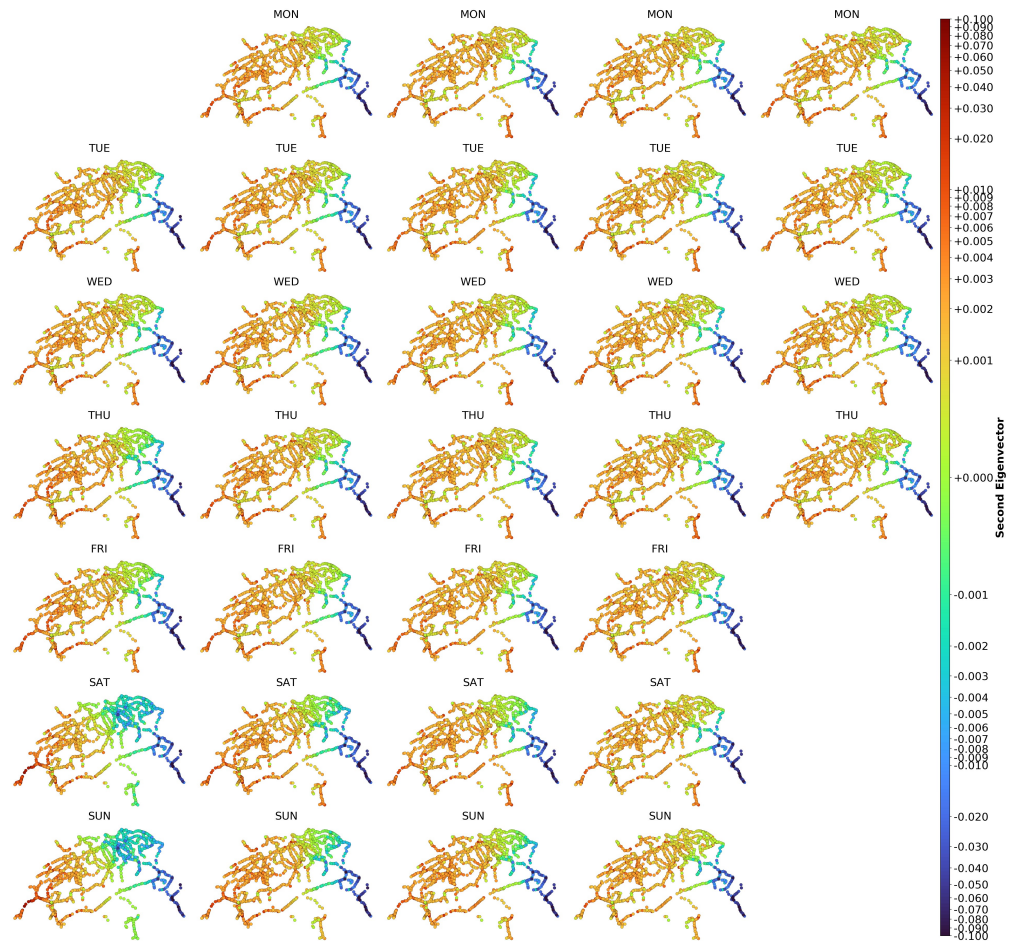


Figure 4. Spectral clustering in space and time (2nd Eigenvector)

Spatio-temporal dynamics of the the Swiss railway network's weakly-connected sub-communities in October 2019. There is a stark displacement of the border between groups of states in the first weekend that attenuates gradually in the following weeks.

Our results are in agreement with the theoretical foundation [7], according to which the eigenvector associated with the second eigenvalue of a Markov chain can be used to detect nearly disconnected groups of states. This is clearly the case for the southeastern canton of Grisons where we also have a jurisdictional separation. Surprisingly enough, under consideration of the actual flows, the weakly-connected sub-communities are not static and a spatio-temporal shift in the spectral clustering is possible. What was barely visible from the stationary distribution, becomes obvious with the second eigenvector, namely the fact that the first weekend of October developed a completely distinct dynamic which might be related to the beginning of the Swiss autumn holidays.

Perturbation analysis

In order to calculate the corresponding systemic risk measures, we performed daily perturbation analyses for all the stations of our network. By comparing the respective stationary distributions, before and after perturbation of a certain station, one obtains a very detailed picture of the spatio-temporal dynamics. As an example, we can see the countrywide effect on π by a disruption at Bern in Fig 5. We strongly believe that such functionality can be best demonstrated as an interactive web application and because of that we invite the reader to work with the open-source code in our online repository¹.

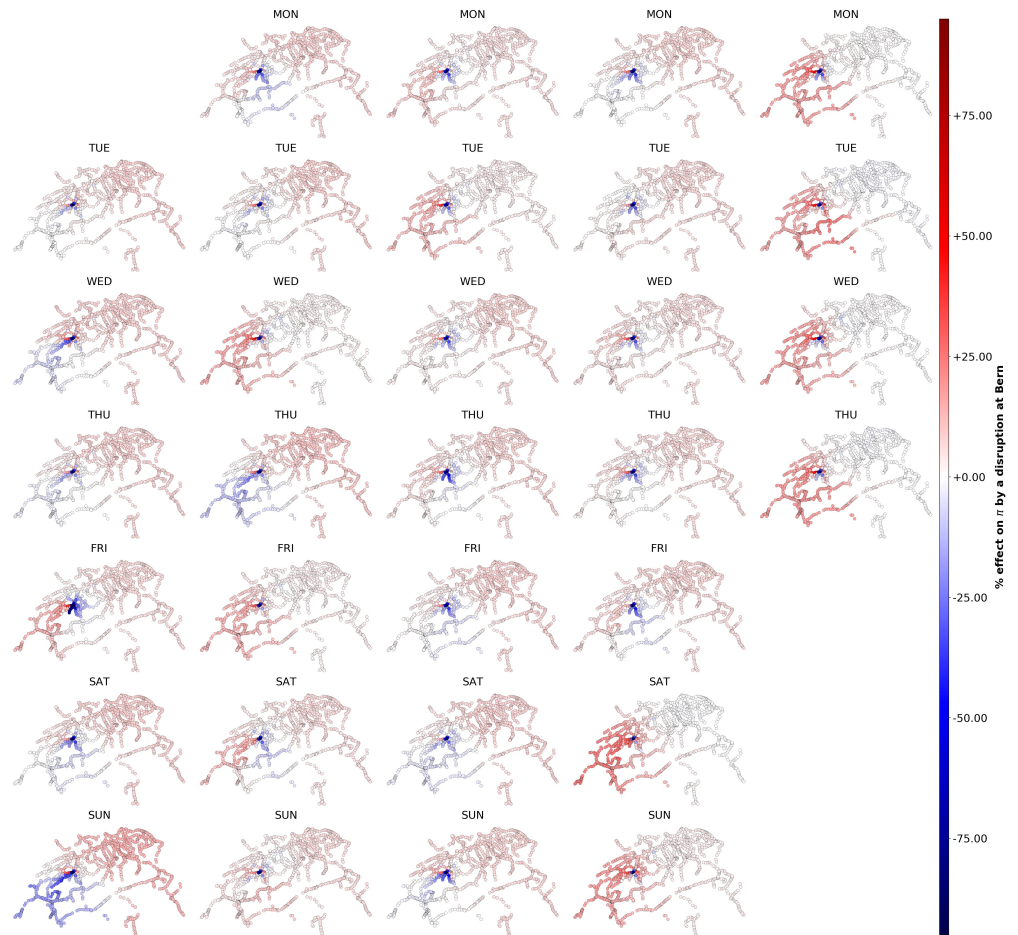


Figure 5. Countrywide effect on π by a disruption at Bern

Values are percentages of change with respect to the stationary distribution of the corresponding day. Positive changes can be understood as increased traffic, negative changes as reduced traffic. The last week of October appears to have a stable behavior.

Overall, with the exception of the more consistent last week, the day-to-day behavior of the system appears almost weather-like. The effects spread in an asymmetric and fragmented manner as certain routes seem to be more affected than others that remain largely neutral despite their geographic proximity to the disrupted station. Positive effect suggests traffic above normal capacity and high congestion as the probability of staying at certain stations rises. Negative effect means reduced traffic as the respective stations operate below normal capacity, but it also means reduced accessibility.

¹<https://bit.ly/3fGvCXC>

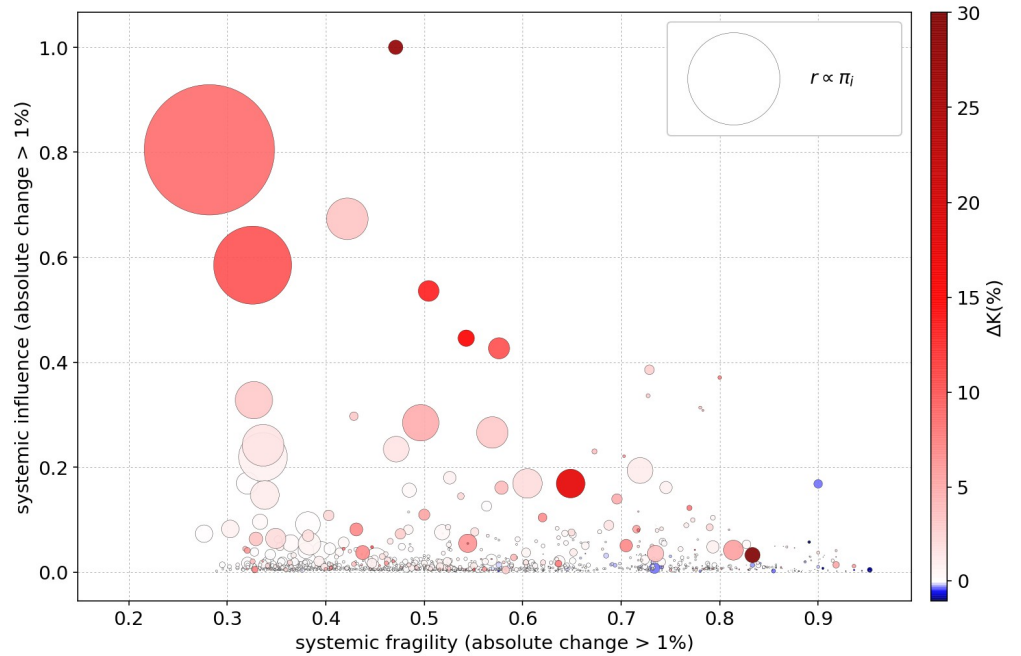
Global and local systemic risk measures

Known network measures, such as various centrality measures [8, 13, 21], are purely based on network structure and often fail to address dynamic aspects of flow and time which are crucial when evaluating the real behaviour of the system and the related risks. To study these dynamics, we model the network as a nonlinear high dimensional spatio-temporal system with a series of MCs and accordingly employ time series of systemic risk measures, which primarily come from an econometric context [2].

As suggested previously, a global measure of network performance is provided by the Kemeny constant. If we compare the respective values of K for every station, before and after disruption, we get the local measure ΔK [7, 16, 17]. Given some perturbed matrix $\tilde{\mathbb{P}}$ and the original \mathbb{P} , $\Delta K = \frac{K(\tilde{\mathbb{P}}) - K(\mathbb{P})}{K(\mathbb{P})}$.

Positive ΔK means deterioration of the overall network performance when the node is disrupted. In this case, ΔK is clearly a systemic risk measure. On the other hand, negative ΔK means improvement of the overall network performance when the node is disrupted. This is known in traffic planning as the *Braess Paradox* [5], blue in Fig 6.

Figure 6. ΔK , systemic influence and systemic fragility of each station
Median values of ΔK , systemic influence and systemic fragility of all common stations over a period of one month. The most disruptive stations are not the biggest ones.



Systemic Influence and *Systemic Fragility*, Fig 6, are dedicated systemic risk measures that were first introduced in [2] and further developed in [17]. For a given threshold γ , we define the absolute impact of a disrupted node i on some node $j \neq i$ as

$$W_{ij} = \begin{cases} |\tilde{\pi}_j - \pi_j|, & \text{if } \frac{|\tilde{\pi}_j - \pi_j|}{\pi_j} > \gamma \\ 0, & \text{otherwise} \end{cases} \quad \text{and the systemic influence as } I_i = \frac{\sum_j W_{ij}}{\max_j \sum_j W_{:j}}$$

$$\text{Systemic fragility is then defined as } \phi_i = \frac{\sum_j F_{ji}}{\max_j \sum_j F_{:j}}, \quad \text{where } F_{ji} = \begin{cases} 1, & \text{if } W_{ji} > 0 \\ 0, & \text{otherwise} \end{cases}$$

Dynamics of the system in time

Best and worst case assessments, spatio-temporal community detection and identification of critical stations can be facilitated with the use of descriptive statistics. Simple indicators, such as minimum, maximum, median and standard deviation, efficiently summarize the trends on an aggregate level and highlight areas that require closer attention, both important criteria for experts and decision makers alike.

We identified 7 measures that best capture the temporal dynamics of the system: inflow, outflow, π (stationary distribution), weakly-connected sub-communities, ΔK , systemic influence and systemic fragility. Inflow and outflow, which are the respective frequencies of inbound and outbound trains for each node, were found to be practically identical for the Swiss railway network. Because this might not be the case for other systems, we don't consider the measures as redundant, Fig 7.

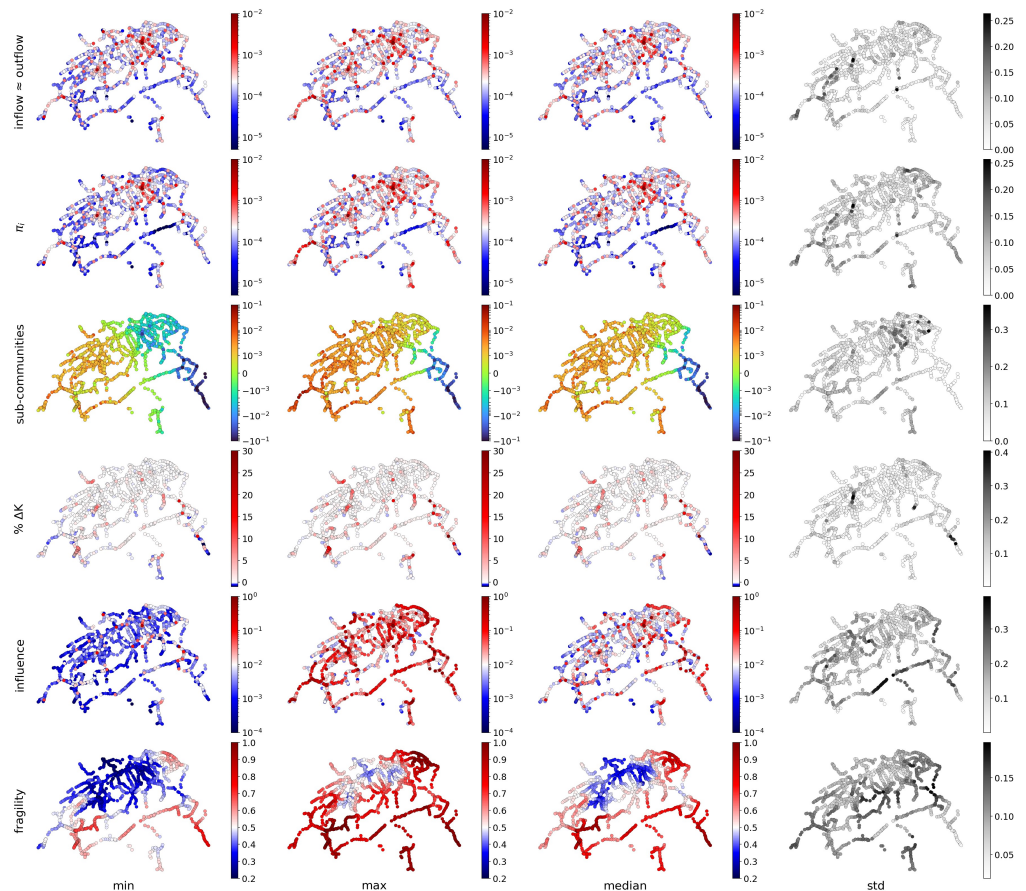


Figure 7. Descriptive statistics of the selected measures over one month

In contrast to systemic influence, the patterns ensuing from systemic fragility are remarkably continuous. Of particular interest is the area around Olten in central Switzerland, which is known to host the *null-point* stone of the Swiss railway network. The area displays high resistance to perturbations even at maximum fragility. There is historical evidence [3] that this part of the network belonged to the Swiss Central Railways (SCB), a 19th century company that was founded with the primary goal to construct a railway cross with its center at Olten. This is a striking finding that suggests a **link between systemic fragility and network growth**, a claim which needs to be verified also for other networks in further research.

Rankings

We conclude the presentation of our results with some rankings. The complementary character of the selected measures becomes clear when we consider the top 10 stations of the respective high and low segments, Fig 8.

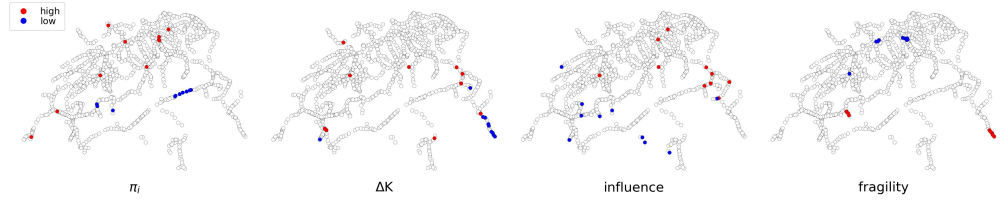


Figure 8. Highest and lowest values of selected measures, 1 month median
Each of the above metrics captures unique qualities of the system.

Table 2 lists the top 10 stations with highest positive impact on Kemeny constant. Their position, suggests that, when a disruption occurs, certain dependent groups of states without re-routing alternatives, become almost disconnected from the main body. This explains why very central stations in areas with multiple re-routing alternatives do not necessarily have the highest positive effect on K .

Table 2. Top 10 stations with highest positive $\Delta K(\%)$, 1 month median

Rank	Name	π_i	$\Delta K(\%)$	influence	fragility
1	Pontresina	0.001124	30.255355	0.032478	0.833333
2	Sargans	0.001063	27.812951	1.000000	0.471014
3	Bellinzona	0.002121	17.818407	0.168668	0.648649
4	Chur	0.001216	15.010850	0.445668	0.542636
5	Landquart	0.001537	13.356088	0.535641	0.504505
6	Arth-Goldau	0.001567	10.511559	0.426408	0.575949
7	Courtételle	0.000224	10.138158	0.047553	0.446970
8	Bern	0.005762	10.112646	0.584837	0.325758
9	Aigle-Hôpital	0.000108	10.076081	0.042331	0.774775
10	Les Arnoux	0.000094	9.558433	0.005585	0.801802

Table 3 lists the top 10 stations with highest negative impact on Kemeny constant. In accordance to the Braess paradox, a disruption at one of these nodes, improves the overall network performance. The metric favors a more circular network by penalizing extremities and should not be a panacea for real planning decisions.

Table 3. Top 10 stations with highest negative $\Delta K(\%)$, 1 month median

Rank	Name	π_i	$\Delta K(\%)$	influence	fragility
1	Bernina Diavolezza	0.000207	-1.260966	0.057206	0.890909
2	Cavaglia	0.000165	-0.792631	0.007344	0.904762
3	Campocologno	0.000362	-0.768361	0.004253	0.952381
4	Tirano	0.000080	-0.751423	0.002468	0.944444
5	Cadera	0.000087	-0.681906	0.005925	0.904762
6	Brusio	0.000200	-0.648663	0.004372	0.952381
7	Miralago	0.000124	-0.385095	0.003973	0.936508
8	Champéry-Village	0.000042	-0.376263	0.001163	0.882883
9	Litzirüti	0.000167	-0.343973	0.002103	0.575540
10	Morteratsch	0.000155	-0.306009	0.019862	0.886792

Table 4 lists the top 10 most influential stations. Sargans, which has a neuralgic position right at the junction (or minimal cut) between the two major sub-components, is by far the most influential, surpassing Zürich HB, the most frequented station.

Table 4. Top 10 stations with highest systemic influence, 1 month median

Rank	Name	π_i	$\Delta K(\%)$	influence	fragility
1	Sargans	0.001063	27.812951	1.000000	0.471014
2	Zürich HB	0.009634	8.509657	0.804672	0.281818
3	Winterthur	0.003072	3.411224	0.673169	0.421875
4	Bern	0.005762	10.112646	0.584837	0.325758
5	Landquart	0.001537	13.356088	0.535641	0.504505
6	Chur	0.001216	15.010850	0.445668	0.542636
7	Arth-Goldau	0.001567	10.511559	0.426408	0.575949
8	Klosters Platz	0.000711	2.777364	0.385454	0.728682
9	Filisur	0.000275	7.356629	0.370642	0.800000
10	Reichenau-Tamins	0.000293	2.825486	0.336020	0.727273

Table 5 lists the top 10 stations with highest systemic fragility. If fragility is actually related to network growth, a claim that requires additional empirical and theoretical evidence, then these stations are very fragile branches of a growing tree. To this end, high systemic fragility might imply growth potential.

Table 5. Top 10 stations with highest systemic fragility, 1 month median

Rank	Name	π_i	$\Delta K(\%)$	influence	fragility
1	Campocologno	0.000362	-0.768361	0.004253	0.952381
2	Campascio	0.000109	-0.283120	0.002450	0.952381
3	Brusio	0.000200	-0.648663	0.004372	0.952381
4	Tirano	0.000080	-0.751423	0.002468	0.944444
5	Miralago	0.000124	-0.385095	0.003973	0.936508
6	Le Prese	0.000272	5.695729	0.011444	0.936364
7	Boden	0.000051	-0.110071	0.001573	0.927928
8	Matten	0.000051	0.640186	0.001893	0.927928
9	St. Stephan	0.000051	1.691439	0.001943	0.927928
10	Stöckli	0.000051	2.929745	0.002014	0.918919

Conclusion

StationRank provides a comprehensive data-driven methodology for spatio-temporal analysis and evaluation of actual railway dynamics. The respective data set is updated on a daily basis, so given the simplicity and efficiency of the algorithm, it is very easy to achieve near real-time results. Every day, a preprocessed corpus is generated from the raw data, the respective MC is built and subsequently perturbed to account for a linearly variable disruption at each station of the network. Depending on the scope of application, the results can be used in the form of interactive perturbation analyses, holistic spatio-temporal evaluations of the system's behavior and of course various rankings, thus enabling valuable insights.

Acknowledgments

The corresponding author would like to thank Mirjam Petri for the preliminary discussions on the topic. The authors would like to thank the Swiss Federal Railways (SBB) for daily collecting, maintaining and publishing the actual data.

References

1. Absorbing Markov Chains. Brilliant.org; Available from: <https://brilliant.org/wiki/absorbing-markov-chains/>.
2. Battiston S, Puliga M, Kaushik R, Tasca P, Caldarelli G. DebtRank: Too Central to Fail? Financial Networks, the FED and Systemic Risk. *Scientific Reports*. 2012;2(1):541. doi:10.1038/srep00541.
3. Bärtschi HP. Schweizerische Centralbahn (SCB); 2011. Available from: <https://hls-dhs-dss.ch/de/articles/041892/2011-10-27/>.
4. Berche B, von Ferber COO, Holovatch T, Holovatch Y. Public Transport Networks under Random Failure and Directed Attack. *DySES*. 2010;2.
5. Braess D, Nagurney A, Wakolbinger T. On a Paradox of Traffic Planning. *Transportation Science*. 2005;39(4):446–450. doi:10.1287/trsc.1050.0127.
6. Büchel B, Corman F. The disruption at Rastatt and its effects on the Swiss railway system. In: Peterson A, Joborn M, Bohlin M, editors. RailNorrköping 2019. 8th International Conference on Railway Operations Modelling and Analysis (ICROMA), Norrköping, Sweden, June 17th – 20th, 2019. vol. 69 of Linköping Electronic Conference Proceedings. Linköping: Linköping University Electronic Press; 2019-09-13. p. 221 – 238.
7. Crisostomi E, Kirkland S, Shorten R. A Google-like model of road network dynamics and its application to regulation and control. *International Journal of Control - INT J CONTR*. 2011;84:633–651. doi:10.1080/00207179.2011.568005.
8. Dorbritz R. Methodology for assessing the structural and operational robustness of railway networks. ETH Zurich. Zurich; 2012.
9. Doytchinov B, Irby R. Time Discretization of Markov Chains. *Pi Mu Epsilon Journal*. 2010;13(2):69–82.
10. Erath A, Löchl M, Axhausen KW. Graph-Theoretical Analysis of the Swiss Road and Railway Networks Over Time. *Networks and Spatial Economics*. 2009;9(3):379–400. doi:10.1007/s11067-008-9074-7.
11. Ist-Daten (actual data). SBB; 2019. Available from: <https://opentransportdata.swiss/de/dataset/istdaten>.
12. İsmail Şahin. Markov chain model for delay distribution in train schedules: Assessing the effectiveness of time allowances. *Journal of Rail Transport Planning & Management*. 2017;7(3):101 – 113. doi:<https://doi.org/10.1016/j.jrtpm.2017.08.006>.
13. Kurant M, Thiran P. Extraction and analysis of traffic and topologies of transportation networks. *Physical review E, Statistical, nonlinear, and soft matter physics*. 2006;74:036114. doi:10.1103/PhysRevE.74.036114.

14. Liu N, Stewart WJ. Markov Chains and Spectral Clustering. In: Hummel KA, Hlavacs H, Gansterer W, editors. Performance Evaluation of Computer and Communication Systems (PERFORM). vol. LNCS-6821 of Performance Evaluation of Computer and Communication Systems. Milestones and Future Challenges. Vienna, Austria: Springer; 2010. p. 87–98. Available from: <https://hal.inria.fr/hal-01586907>.
15. Markov AA. An Example of Statistical Investigation of the Text Eugene Onegin Concerning the Connection of Samples in Chains. *Science in Context*. 2006;19(4):591–600. doi:10.1017/s0269889706001074.
16. Moosavi V, Hovestadt L. Modeling Urban Traffic Dynamics in Coexistence with Urban Data Streams. In: Proceedings of the 2Nd ACM SIGKDD International Workshop on Urban Computing. UrbComp '13. New York, NY, USA: ACM; 2013. p. 10:1–10:7. Available from: <http://doi.acm.org/10.1145/2505821.2505822>.
17. Moosavi V, Isacchini G. A Markovian model of evolving world input-output network. *PLOS ONE*. 2017;12(10):1–18. doi:10.1371/journal.pone.0186746.
18. Page L, Brin S, Motwani R, Winograd T. The PageRank Citation Ranking: Bringing Order to the Web. Stanford InfoLab; 1999. 1999-66. Available from: <http://ilpubs.stanford.edu:8090/422/>.
19. Porta S, Crucitti P, Latora V. The network analysis of urban streets: A dual approach. *Physica A: Statistical Mechanics and its Applications*. 2006;369(2):853–866. doi:<https://doi.org/10.1016/j.physa.2005.12.063>.
20. Transience and Recurrence of Markov Chains. Brilliant.org; Available from: <https://brilliant.org/wiki/transience-and-recurrence/>.
21. Wei S, Teng SN, Li HJ, Xu J, Ma H, Luan Xl, et al. Hierarchical structure in the world's largest high-speed rail network. *PLOS ONE*. 2019;14(2):1–11. doi:10.1371/journal.pone.0211052.